Krishna Garikipati
Ellen M. Arruda
Editors

IUTAM Bookseries

IUTAM Symposium on Cellular, Molecular and Tissue Mechanics

Proceedings of the IUTAM Symposium held at Woods Hole, Mass., USA, June 18–21, 2008

Springer

Krishna Garikipati • Ellen M. Arruda
Editors

IUTAM Symposium on Cellular, Molecular and Tissue Mechanics

Proceedings of the IUTAM symposium
held at Woods Hole, Mass., USA,
June 18–21, 2008

Springer

IUTAM BOOKSERIES

Volume 16

Aims and Scope of the Series

The IUTAM Bookseries publishes the proceedings of IUTAM symposia under the auspices of the IUTAM Board.

For other titles published in this series, go to
www.springer.com/series/7695

Editors
Krishna Garikipati
Dept. Mechanical Engineering
University of Michigan
Ann Arbor, Michigan
USA
krishna@umich.edu

Ellen M. Arruda
Dept. Mechanical Engineering
University of Michigan
Ann Arbor, Michigan
USA
arruda@umich.edu

ISSN 1875-3507 e-ISSN 1875-3493
ISBN 978-90-481-3347-5 e-ISBN 978-90-481-3348-2
DOI 10.1007/978-90-481-3348-2
Springer Dordrecht Heidelberg London New York

Library of Congress Control Number: 2009938830

Cover design: eStudio Calamar S.L.

Printed on acid-free paper

Springer is part of Springer Science+Business Media (www.springer.com)

Elastic and Electrostatic Model for DNA in Rotation–Extension Experiments

S. Neukirch, N. Clauvelin, and B. Audoly

Abstract We present a self-contained theory for the mechanical response of DNA in extension–rotation single molecule experiments. The theory is based on the elasticity of the double-helix and the electrostatic repulsion between two DNA duplex. The configuration of the molecule at large imposed rotation is assumed to comprise two phases, linear and superhelical DNA. Thermal fluctuations are accounted for in the linear phase and electrostatic repulsion is treated in the superhelical phase. This analytical model enables the computation of the supercoiling radius and angle of DNA during experiments. The torsional stress in the molecule and the slope of the linear region of the experimental curve are also predicted and compared successfully with experimental data.

1 Introduction

Mechanics of the DNA molecule is a key component for several biological processes at the cellular level. The action of enzymes and proteins on DNA has been found to often depend on the mechanical stress present in the molecule. In this context single molecule experiments, where forces and torques are applied onto individual DNA molecules, offer a remarkable opportunity to study mechanical issues. We are here interested in extension–rotation experiments performed with the help of optical or magnetic tweezers [2, 3, 6, 17]. Although different experimental methods exist, within a mechanical point of view the problem is the same: a dsDNA molecule is fixed by one end on a glass cover-slip while the other end is attached to a mechanical system that exerts a pulling force and a torsional moment on the molecule. Experiments are carried out at constant pulling force while the upper end of the molecule is rotated. The imposed rotation is characterized by the number of turns n

S. Neukirch (✉), N. Clauvelin, and B. Audoly
CNRS and UPMC Univ Paris 06, UMR 7190, IJLRDA, 4, Place Jussieu,
Paris F-75005, France
e-mail: firstname.lastname@upmc.fr

K. Garikipati and E.M. Arruda (eds.), *IUTAM Symposium on Cellular, Molecular and Tissue Mechanics*, IUTAM Bookseries 16, DOI 10.1007/978-90-481-3348-2_10,

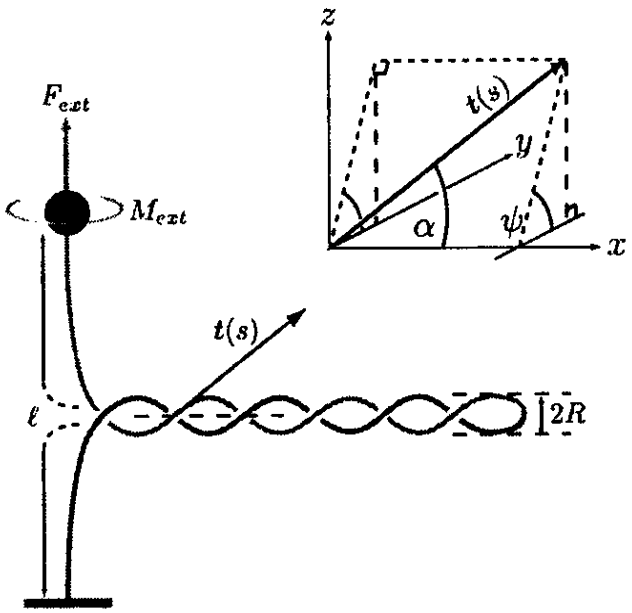

Fig. 1 Sketch of the magnetic tweezers experiment. A B-DNA molecule of total contour length ℓ is fixed in $s = 0$ to a glass surface while the other end in $s = \ell$ is attached to a magnetic bead. A magnet is used to pull and impose a $2\pi n$ rotation on the bead. As a result the molecule is subject to a pulling force F_{ext} and a torque M_{ext}. The superhelical angle and radius are denoted α and R respectively. The zenith angle α and the azimuth angle ψ of the tangent vector with regard to the superhelical axis $\mathbf{e}_x$ are also shown

performed. DNA is then under or over-wound and various molecule conformations are observed [3]. In the present study we focus on the over-winding of a dsDNA molecule for large imposed rotations. In such cases the molecule wraps around itself in a helical way and forms plectonemes as shown in Fig. 1.

Plectonemic DNA mechanics requires to account for various physical effects such as thermal fluctuations, electrostatic interactions, self-avoidance, and DNA elasticity. Although several studies have addressed these issues, a model considering all these effects together is still lacking. For instance, Goyal et al have presented in [8?] a numerical model which addresses within a mechanical point of view the formation of DNA supercoils. Coleman and Swigon give in [5] an accurate description of the mechanical equilibrium of supercoiled elastic rods. However their model was applied to DNA plasmids, and does not take into account either thermal fluctuations or DNA–DNA long-range interactions. More recently Purohit has addressed plectonemic DNA mechanics using Kirchhoff elastic rod theory, although contact forces in the plectonemic part of the molecule are not taken into account [14]. Marko has presented an analytical, though not self-contained, model which fit experimental data with good agreement [10]. This model accounts for thermal fluctuations and self-avoidance but relies on numerical results extracted from Monte–Carlo simulations.

The present paper is an extension of our previous analysis of plectonemic DNA mechanics [4]. We present an analytical model for the mechanical response of plectonemic DNA in extension–rotation experiments. We focus on the plectonemic

regime, which means we consider large imposed rotations (large n). Our elastic model accounts for DNA–DNA interactions present in the plectonemic region and for thermal fluctuations present in the tails region.

2 Model

The present model investigates the equilibrium behavior of an elastic rod with bending rigidity K_0 (the bending persistence length is $A = K_0/(k_B T)$, where k_B is the Boltzmann constant and T the absolute temperature) and twisting rigidity K_3 under traction and torsion as shown in Fig. 1. This is a coarse-grained model for DNA where base-pairs details are neglected. For instance, the anisotropic flexibility of the molecule, originating from base pairing and major–minor groove geometry, is smoothed out at a scale of several base pairs.

2.1 Geometry

We start with a geometric description of the rod configurations relevant to the plectonemic regime. This defines a reduced set of configurations (Ansatz), over which we shall minimize the elastic strain energy associated with deformations. The rod, of length ℓ, is considered inextensible and has circular cross-section; let s denote the arclength along the rod. The strain energy involves, at lowest order, the geometric curvature $\kappa(s)$ of the centerline of the rod as well as the twist $\tau(s)$. The rod centerline is parameterized by $\mathbf{r}(s)$ and its unit tangent $\mathbf{t} \stackrel{\text{def}}{=} \mathrm{d}\mathbf{r}/\mathrm{d}s$ can be described with spherical angles, as shown in Fig. 1: $\alpha(s)$ is the zenith angle and $\psi(s)$ the azimuth angle with respect to the direction $\mathbf{e_x}$ along the common axis of the two superhelices in the plectonemic region.

We consider the following configurations, relevant to a large applied number of turns, n. The tails are assumed to be straight but twisted (thermal fluctuations will be accounted for by using the rescaled tail length predicted by the worm-like chain [WLC] theory). The plectonemes are described by two identical and uniform helices where each of these helices is itself a double-stranded DNA molecule. Both the end loop of the plectonemes and the matching region between the tails and the plectonemic part are neglected. Consequently the rod comprises two phases: one made up of straight and twisted tails and the other one of plectonemic structures. In the tails the rod is aligned with the $\mathbf{e_z}$ axis: $\mathbf{t} = \mathbf{e_z}$. The geometric curvature $\kappa \stackrel{\text{def}}{=} |\mathrm{d}\mathbf{t}/\mathrm{d}s|$ is zero, $\kappa(s) = 0$. In each filament of the plectonemes, the position vector $\mathbf{r}(s)$ and the tangent vector $\mathbf{t}(s)$ describe a superhelix of axis $\mathbf{e_x}$:

$$\begin{cases} r_x(s) = s\cos\alpha \\ r_y(s) = \chi R \sin\psi(s) \\ r_z(s) = -\chi R \cos\psi(s) \end{cases} \quad \text{and} \quad \begin{cases} t_x(s) = \cos\alpha \\ t_y(s) = \sin\alpha\cos\psi(s) \\ t_z(s) = \sin\alpha \sin\psi(s) \end{cases} \tag{1}$$

The other filament of the plectonemes is obtained by a rotation of 180° around the axis $\mathbf{e}_x$. Here $\chi = \pm 1$ stands for the chirality of the two (super-)helices – for example in Fig. 1, $\chi = -1$. The quantities R and α are the superhelical radius and angle, respectively. In Eq. 1, the condition $\mathrm{d}\mathbf{r}/\mathrm{d}s = \mathbf{t}$ yields $\mathrm{d}\psi/\mathrm{d}s = \chi \sin\alpha/R$. The curvature in the plectonemes is $\kappa(s) = |\mathrm{d}\mathbf{t}/\mathrm{d}s| = \frac{\sin^2\alpha}{R}$. Noting ℓ_p the contour length spent in the plectonemes, we obtain the following expression for the integral of the squared curvature over the whole length of the rod $\int_0^\ell \kappa^2\,\mathrm{d}s = \frac{\sin^4\alpha}{R^2}\,\ell_\mathrm{p}$. The end torque twists the filament. For a rod with circular cross-section, the twist $\tau(s)$ at equilibrium is uniform, $\mathrm{d}\tau/\mathrm{d}s = 0$ for all s, so we have $\int_0^\ell \tau^2\,\mathrm{d}s = \tau^2\ell$. In conclusion the equilibrium configuration of the rod is fully specified by the centerline, through the variables α, R and ℓ_p, and an additional scalar τ describing twist. The twist τ is geometrically related to the number of turns imposed on the magnetic bead, n, which is equal to the link of the DNA molecule, $n = \mathrm{Lk}$. In the present case the link reads [13]:

$$\mathrm{Lk} = \mathrm{Tw} + \mathrm{Wr} = \frac{1}{2\pi}\int_0^\ell \tau\,\mathrm{d}s - \chi\,\frac{\sin 2\alpha}{4\pi\,R}\,\ell_p = \frac{1}{2\pi}\left(\tau\,\ell - \chi\,\frac{\sin 2\alpha}{2\,R}\,\ell_\mathrm{p}\right), \quad (2)$$

as we neglect the writhe of the tails.

2.2 *Energy Formulation*

Using the above notations the rod is described by four variables: α the superhelical angle, R the superhelical radius, τ the twist and ℓ_p the contour length spent in the plectonemes. We proceed to derive the total energy of the system as a function of these four variables. It is the sum of three terms, $V = V_\mathrm{el} + V_\mathrm{ext} + V_\mathrm{int}$, where the first term is the strain elastic energy, the second is the potential energy associated with the external loads F_ext and M_ext, and the third accounts for interaction of the filaments in the plectonemes. The strain elastic energy for the rod of total contour length ℓ is $V_\mathrm{el} = \frac{K_0}{2}\int_0^\ell \kappa^2\,\mathrm{d}s + \frac{K_3}{2}\int_0^\ell \tau^2\,\mathrm{d}s = \frac{K_0}{2}\frac{\sin^4\alpha}{R^2}\ell_p + \frac{K_3}{2}\tau^2\ell$. This strain energy is to be seen as the first order approximation of a more comprehensive strain energy, as for example terms for the longitudinal extension of the molecule or terms coupling extension and twist could be added. Nevertheless in rod theory extension (and shear) are higher order when compared to bending and twisting and indeed stretching experiments on DNA have reported a large (>1,000 pN) stretching stiffness [19]. We do not take into account the reduction of the effective torsional rigidity in the tails due to fluctuations [12]. The potential energy associated with the pulling force is given by $V_\mathrm{ext} = -F_\mathrm{ext}(z(\ell) - z(0)) \overset{\mathrm{def}}{=} -F_\mathrm{ext}\,\Delta z$, where $\Delta z = \ell - \ell_p$ for straight tails. There is no term associated with the external moment since the rotation n rather than the moment is imposed. The DNA–DNA interactions that occurs in the plectonemic region of the rod involves different effects depending on the values of the supercoiling radius R. At moderate to large values of R (i.e., several nm)

electrostatics effects dominate. In contrast to our previous paper [4], we here take these electrostatics interactions into account. We introduce an energy of interaction per unit length of molecule for the plectonemic phase, $U(R, \alpha)$ which is assumed to depend on the superhelical radius and angle only $V_{int} = \ell_p U(R, \alpha)$.

Finally we obtain the following function for the total energy of the system:

$$V(R, \alpha, \ell_p, \tau) = \frac{K_0}{2} \frac{\sin^4 \alpha}{R^2} \ell_p + \frac{K_3}{2} \tau^2 \ell - F_{\text{ext}} (\ell - \ell_p) + \ell_p U(R, \alpha) , \quad (3)$$

subjected to the end rotation constraint $n = Lk$ where Lk is given by Eq. 2. As this constraint is linear in ℓ_p we use it in order to substitute ℓ_p with an expression involving τ and n. Dropping the constant term $-F_{\text{ext}}\ell$, we obtain:

$$\begin{aligned} V(\alpha, R, \tau) &= \frac{K_3}{2} \tau^2 \ell + (2\pi n - \tau \ell) \left[\frac{-2\chi}{\sin 2\alpha} \left(\frac{K_0 \sin^4 \alpha}{2R} + RF_{\text{ext}} + RU(R, \alpha) \right) \right] \\ &= \frac{K_3}{2} \tau^2 \ell + g(\tau) f(R, \alpha) . \end{aligned} \quad (4)$$

2.3 *Ubbink and Odijk Model of DNA–DNA Interactions*

In their study of supercoiled DNA plasmids [18] Ubbink and Odijk derive an analytical expression for the electrostatic interaction energy between two interwound DNA molecules. Their work is based on the Poisson-Boltzmann theory where, in the computation of the electrostatic repulsion of the two charged molecules, the presence and fluctuations of the counter-ions and co-ions in solution play an important role. The electrostatic interaction energy (per unit length) derived in [18] writes as follow:

$$U(R, \alpha) = \frac{1}{2} k_B T \nu^2 l_B \sqrt{\frac{\pi}{\kappa R}} e^{-2\kappa R} \varphi(\alpha) \quad (5)$$

where k_B is the Boltzmann constant, T the temperature in Kelvin, ν the effective linear charge density (in m^{-1}), l_B the Bjerrum length, and κ^{-1} the Debye length. For a typical temperature $T = 300$ K we have $l_B = 0.7$ nm, and for a monovalent salt concentration $c = 10$ mM the Debye length is $\kappa^{-1} = 3.07$ nm. The value of the effective charge ν depends on the salt concentration. For a monovalent salt concentration $c = 10$ mM, we have $\nu = 1.97\ \text{nm}^{-1}$. The winding of the two molecules is rendered by the function $\varphi(\alpha) = 1 + 0.83 \tan^2 \alpha + 0.86 \tan^4 \alpha$ which introduces a dependance of U on the superhelical angle α.

2.4 Equilibrium Equations

The total energy of the system, Eq. 4, which takes into account the constraint related to the imposed end rotation, is now minimized with respect to its three variables in order to obtain equations for the mechanical response of the DNA molecule. The first step in the minimization is to consider the Euler-Lagrange equations (first variation of V): $(\partial V/\partial\alpha,\ \partial V/\partial R,\ \partial V/\partial\tau) = 0$, which yields:

$$2K_0\frac{\cos\alpha\,\sin^3\alpha}{R^2} + \frac{\partial U}{\partial\alpha} - \frac{2}{\tan 2\alpha}\left(\frac{K_0}{2}\frac{\sin^4\alpha}{R^2} + F_{\text{ext}} + U(R,\alpha)\right) = 0, \quad (6)$$

$$F_{\text{ext}} - \frac{K_0}{2R^2}\sin^4\alpha + R\frac{\partial U}{\partial R} + U(R,\alpha) = 0, \quad (7)$$

$$M_{\text{ext}} + \chi\frac{2R}{\sin 2\alpha}\left(\frac{K_0}{2}\frac{\sin^4\alpha}{R^2} + F_{\text{ext}} + U(R,\alpha)\right) = 0. \quad (8)$$

This is a system of three equations with three unknowns (α, R, M_{ext}). The use of $M_{\text{ext}} = K_3\,\tau$ instead of τ in the last equilibrium equation renders the set of equations independent of K_3. For a given potential $U(R,\alpha)$ these equilibrium equations may have several solutions and the number of solutions may depend on the value of the force F_{ext}. In the case of the potential we use in this work, there are in fact two solutions at low force and these two solutions collapse and vanish for a certain force threshold, typically several pico Newton (see Section 3). We therefore examine the stability of the two concurrent solutions by computing the second variation of the potential function $V(\alpha, R, \tau)$. The second derivatives of V are ordered in a 3x3 matrix, called the Hessian matrix:

$$H = \begin{bmatrix} \partial_{\alpha\alpha}V & \partial_{\alpha R}V & \partial_{\alpha\tau}V \\ \partial_{R\alpha}V & \partial_{RR}V & \partial_{R\tau}V \\ \partial_{\tau\alpha}V & \partial_{\tau R}V & \partial_{\tau\tau}V \end{bmatrix}. \quad (9)$$

The Hessian matrix, once evaluated on the equilibrium solution Eqs. 6, 7, and 8, writes:

$$H|_{\partial V=0} = \begin{bmatrix} g(\tau)\partial_{\alpha\alpha}f & g(\tau)\partial_{\alpha R}f & 0 \\ g(\tau)\partial_{\alpha R}f & g(\tau)\partial_{RR}f & 0 \\ 0 & 0 & K_3\ell \end{bmatrix}. \quad (10)$$

The stability of an equilibrium solution is given by the sign of the eigenvalues (a stable equilibrium requires having only positive eigenvalues). Since $\ell_p > 0$, $g(\tau) > 0$ and then the problem boils down to computing the eigenvalues of the reduced hessian:

$$H|_{\partial V=0} = \begin{bmatrix} \partial_{\alpha\alpha}f & \partial_{\alpha R}f \\ \partial_{\alpha R}f & \partial_{RR}f \end{bmatrix}. \quad (11)$$

Among the two equilibrium solutions, we find that the solution with lower α and R has one negative and one positive eigenvalues, therefore being unstable. The other solution has two positive eigenvalues and is therefore stable: this is the solution we present in the results.

2.5 *Vertical Extension of the Filament*

In extension–rotation experiments the vertical extension of the filament is recorded while the number of turns is increased. The vertical extension of the filament is calculated from Eq. 2 in the following way. First we make the replacement $\ell_p = \ell - \ell_t$. Then in the absence of thermal fluctuations we would write $\ell_t = \Delta z$. Nevertheless we take thermal fluctuations in the tails phase into account by introducing a rescaling factor $\rho_{\text{wlc}} \in [0; 1]$ between the contour length ℓ_t of the tails and their vertical extension $\Delta z = \rho_{\text{wlc}}\, \ell_t$. The factor ρ_{wlc} is computed, following a worm-like chain approach, Eq. 7 in [11]. Finally replacing $\text{Lk} = n$ and solving for Δz yields:

$$\Delta z = \left(1 - \chi \frac{2R}{\sin 2\alpha}\tau\right) \rho_{\text{wlc}}\, \ell + \chi\, \rho_{\text{wlc}} \frac{4\pi R}{\sin 2\alpha} n \,. \tag{12}$$

Note that Eqs. 6 and 7 do not show any n dependence. Consequently the superhelical radius R and angle α, solutions of Eqs. 6 and 7, do not depend on n either. Therefore the vertical extension Δz is a linear function of the number of turns n.

3 Results

For each value of the force F_{ext}, the equilibrium equations, Eqs. 6, 7, and 8, together with an expression for the interaction energy $U(R, \alpha)$ allow one to compute the plectonemic variables α and R and the torsional moment M_{ext}. We compare our results with the model developed in [10] and with experimental data. The comparisons are performed with the same data as in [4, 13]. These data were obtained on a 48 kbp lambda phage DNA molecule in a 10 mM phosphate buffer (see Fig. 2 in [4]) and were kindly provided by V. Croquette (CNRS, France).

3.1 *A Numerical Example*

We give the results of the equilibrium equation for a force value $F_{\text{ext}} = 1.1\text{pN}$. The unstable equilibrium has $R = 0.53\,\text{nm}$, $\alpha = 0.33\,\text{rad}$, and $\tau = 0.11\,\text{rad/nm}$. Once divided by the factor $(k_B T)^2(\ell/K_0)$ (which has dimension of an energy) the reduced hessian matrix, Eq. 11, has $\lambda_1 = 248$ and $\lambda_2 = -6.39$ as eigenvalues

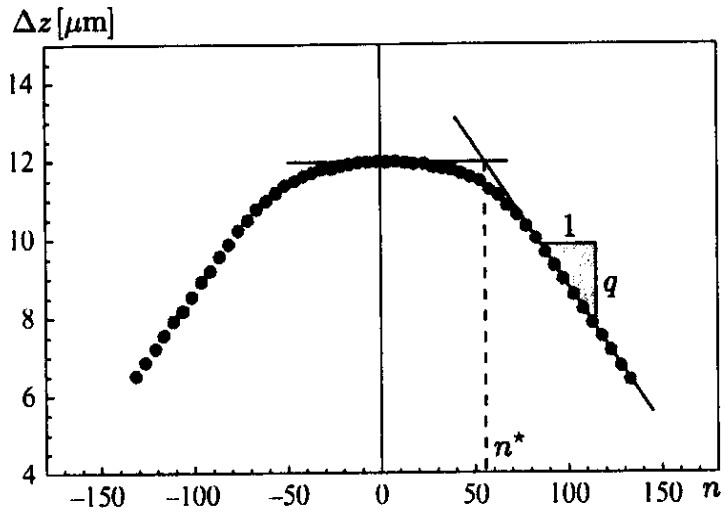

Fig. 2 A typical experimental curve. The slope q is negative (*respectively positive*) for positive (*respectively negative*) n

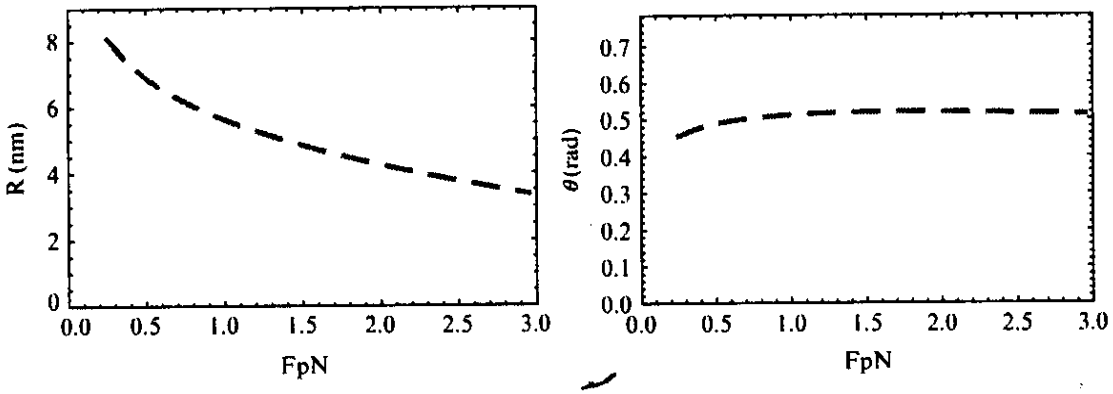

Fig. 3 Values of the superhelical radius R and angle θ as functions of the pulling force F_{ext}

(with R expressed in nm). The stable equilibrium has $R = 5.19\,\text{nm}$, $\alpha = 0.52\,\text{rad}$, $\tau = 0.06\,\text{rad/nm}$, $\lambda_1 = 52.9$ and $\lambda_2 = 0.29$.

The values of R and θ for the stable equilibrium are plotted in Fig. 3 as functions of F_{ext}.

3.2 *Extension–Rotation Curve*

Our model shows that the derivative of the vertical extension Δz with regard to n is constant, i.e., that the extension–rotation curve has a linear part, which is well-known experimentally. The slope q is given by:

$$q = \frac{\mathrm{d}}{\mathrm{d}n}\Delta z = \chi \frac{4\pi R}{\sin 2\alpha}\rho_{wlc} \,. \tag{13}$$

Equation 8 shows that under a positive imposed rotation $n > 0$ (hence a positive torque M_{ext}), $\chi = -1$. Equation 13 then implies that the slope is negative. Alternatively, a negative n means a positive χ and a positive slope, as verified in Fig. 2. The value of the slope q is computed using the values of α and R found by solving the

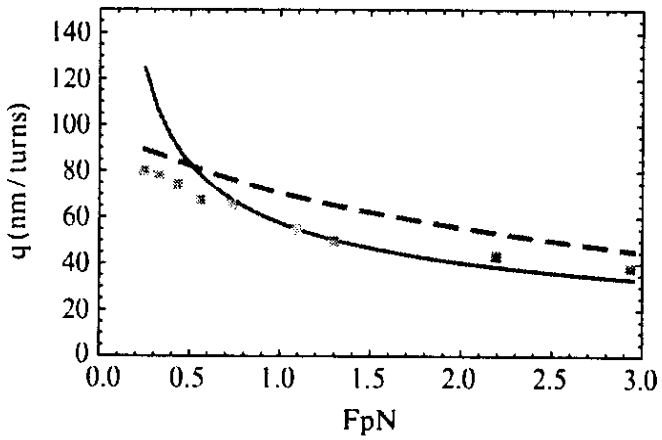

Fig. 4 Slope q of the linear region of extension–rotation curves as a function of the applied force. Our theoretical prediction (*dashed, red*) is compared to experimental data (*green squares*) and to the model in [10] (*continuous, blue*)

equilibrium equations, Eqs. 6, 7, and 8. We plot in Fig. 4 the value of the slope as a function of the force. We also plot the slopes predicted by the model in [10] in order to offer a comparison. Our results show a good quantitative agreement with experimental data. Moreover in comparison with the model in [10], our results follow the experiments in a more consistent manner. We emphasize that the model in [10] uses a free energy for the plectonemic phase that is computed from Monte–Carlo simulations. Furthermore the model assumes a quadratic dependance of the free energy on the linking number, which is not universally valid [9]. In contrast there is no such assumption in our model.

4 Discussion

We have shown in this study that a self-contained mechanical model completed with an analytical description of DNA–DNA long range interactions can reproduce extension–rotation experimental data with good agreement. The principal weakness of our model is that we neglect thermal fluctuations in the plectonemic phase. Investigation of the steepness of the energy in Eq. 4 would give the relative importance of these fluctuations. Another improvement of the present model would be to consider the renormalization of the twist rigidity of the tails due to added link [12].

A possible outcome of this work is the possibility of testing existing descriptions of DNA–DNA interactions. For example the results obtained here with a potential derived from the Poisson-Boltzmann theory could be compared to results obtained with potential derived from the counter-ion condensation theory [16]. Ray and Manning have shown in [15], within the counter-ions condensation theory, the existence of a well in the DNA–DNA interaction energy. If an analytical expression of such an attractive potential was available we might compute interesting effects such as collapse in the plectonemic region [1].

References

1. Bednar J, Furrer P, Stasiak A, Dubochet J, Egelman EH, Bates AD (1994) The twist, writhe and overall shape of supercoiled DNA change during counterion-induced transition from a loosely to a tightly interwound superhelix. Possible implications for DNA structure in vivo. J Mol Biol 235(3):825–847
2. Bustamante C, Macosko JC, Wuite GJL (2000) Grabbing the cat by the tail: Manipulating molecules one by one. Nat Rev Mol Cell Biol 1(2):130–136
3. Charvin G, Allemand JF, Strick T, Bensimon D, Croquette V (2004) Twisting DNA: Single molecule studies. Contemp Phys 45(5):383–403
4. Clauvelin N, Audoly B, Neukirch S (2008) Mechanical response of plectonemic DNA: An analytical solution. Macromolecules 41(12):4479–4483
5. Coleman BD, Swigon D (2004) Theory of self-contact in Kirchhoff rods with applications to supercoiling of knotted and unknotted DNA plasmids. Philos Trans Roy Soc A Math Phys Eng Sci 362(1820):1281–1299
6. Deufel C, Forth S, Simmons CR, Dejgosha S, Wang MD (2007) Nanofabricated quartz cylinders for angular trapping: DNA supercoiling torque detection. Nat Meth 4(3):223–225
7. Goyal S, Perkins NC, Lee CL (2005) Nonlinear dynamics and loop formation in Kirchhoff rods with implications to the mechanics of DNA and cables. J Computat Phys 209(1):371–389
8. Goyal S, Perkins NC, Lee CL (2008) Non-linear dynamic intertwining of rods with self-contact. Int J Non-Linear Mech 43(1):65–73
9. Klenin KV, Vologodskii AV, Anshelevich VV, Dykhne AM, Frank-Kamenetskii MD (1991) Computer simulation of DNA supercoiling. J Mol Biol 217(3):413–419
10. Marko JF (2007) Torque and dynamics of linking number relaxation in stretched supercoiled DNA. Phys Rev E (Statistical, Nonlinear, and Soft Matter Physics) 76(2):021,926
11. Marko JF, Siggia ED (1995) Stretching DNA. Macromolecules 28(26):8759–8770
12. Moroz JD, Nelson P (1997) Torsional directed walks, entropic elasticity, and DNA twist stiffness. Proc Natl Acad Sci USA 94:14, 418
13. Neukirch S (2004) Extracting DNA twist rigidity from experimental supercoiling data. Phys Rev Lett 93(19):198, 107
14. Purohit PK (2008) Plectoneme formation in twisted fluctuating rods. J Mech Phys Solid 56(5):1715–1729
15. Ray J, Manning GS (1994) An attractive force between two rodlike polyions mediated by the sharing of condensed counterions. Langmuir 10(7):2450–2461
16. Stigter D (1995) Evaluation of the counterion condensation theory of polyelectrolytes. Biophys J 69(2):380–388
17. Strick TR, Allemand JF, Bensimon D, Bensimon A, Croquette V (1996) The elasticity of a single supercoiled DNA molecule. Science 271(5257):1835–1837
18. Ubbink J, Odijk T (1999) Electrostatic-undulatory theory of plectonemically supercoiled DNA. Biophys J 76(5):2502–2519
19. Wang MD, Yin H, Landick R, Gelles J, Block SM (1997) Stretching DNA with optical tweezers. Biophys J 72(3):1335–1346